


 Cite this: *Chem. Commun.*, 2023, 59, 7963

 Received 12th April 2023,
Accepted 31st May 2023

DOI: 10.1039/d3cc01802d

rsc.li/chemcomm

Strong circularly polarized luminescence *via* intramolecular excited-state symmetry-breaking charge separation†

 Maria João Álvaro-Martins,^a Chloé Billiaux,^a Pascale Godard,^a Reiko Oda,^b Guillaume Raffy^b and Dario M. Bassani^b*^a

Trans-1,2-di(1-pyrenylamino)cyclohexane was found to display circularly polarized excimer emission ($g_{\text{lum}} = 0.016$) both in polar and non-polar solvents that is assigned to charge separation symmetry breaking on the basis of its large transition state dipole moment (12.1 D).

Organic or inorganic chromophores exhibiting circularly polarized luminescence (CPL) are of interest for numerous applications in sensing, information processing, and anti-counterfeit measures. Their design rests on the incorporation of point, planar,¹ or axial chirality to luminescent chromophores so that the resulting emission possesses non-zero spin angular momentum.² The efficiency of this process can be quantified by the dissymmetry factor, g_{lum} , which is defined as (eqn 1)

$$g_{\text{lum}} = 2 \frac{I_{\text{L}} - I_{\text{R}}}{I_{\text{L}} + I_{\text{R}}}, \quad (1)$$

where I_{L} and I_{R} are the intensities of the left and right CPL, respectively.

The largest values of g_{lum} are generally observed for chiral lanthanide complexes.³ The luminescence from these species is however composed of several sharp lines, not all of which are CPL-active or possess the same CPL sign. In contrast, organic chromophores display a broader mono-signate emission that is more suitable for some applications, but with g_{lum} values that are frequently $\leq 10^{-3}$.^{3,4} The relationship between various chiral groups, emission quantum yield (Φ_{PL}) and g_{lum} for organic chromophores was nicely reviewed by Mori and co-workers.⁵

Experimentally, the largest values of g_{lum} from organic chromophores have been obtained for helicenes⁶ and chiral

cyclophanes.⁷ Good results were also obtained using an axially-chiral quaternaphthalene scaffold appended with polyaromatic dyes displaying locally-excited (LE) or excimer (EX) emission.⁸ Along these lines, intramolecular pyrene excimers have been intensively studied,^{9,10} leading to *e.g.* ion sensing,¹¹ photo-active,¹² or aggregation-enhanced¹³ chiroptical systems.

Efficient CPL originates from non- or partially-allowed electronic transitions according to the observation that it benefits from increasing the magnetic *vs.* the electronic transition dipole moment.^{3,14} In pyrene and pyrene excimers, the lowest-energy radiative transition is symmetry forbidden or possesses a small nuclear overlap integral.¹⁵ One may thus expect that, compared to excimers, charge-separated systems may favor CPL by increasing the spin/charge transfer character of the radiative transition.¹⁴ Indeed, CPL emission from a solution-based chiral exciplex system has recently been reported,¹⁶ and a significant enhancement in CPL emission from a helicene construct featuring a donor-acceptor pair was observed.¹⁷

In addition to readily forming excimers, pyrene derivatives may form emissive exciplexes with charge transfer (CT) character in the presence of various electron donor or acceptor molecules. We thus surmised that small modifications of the redox potential in chiral, pyrene-based bichromophoric systems would lead to CPL from an intramolecular CT state. 1-Aminopyrene is a promising candidate that readily forms CT species because of its high-lying HOMO and H-bonding interactions.¹⁸ *Trans*-1,2-diaminocyclohexane was selected as a chiral platform in view of its ready availability and widespread use in bichromophoric CPL emitters.^{12,13b,19}

Much to our surprise, while investigating the photophysical properties of a symmetric model analogue (compound **1**, Scheme 1), we discovered that its broad, long-wavelength emission possesses a high degree of CT character, indicative of intramolecular charge transfer with strong asymmetry ($g_{\text{lum}} = 0.016$). Based on this, we compared its CT character with that of the previously reported bis-amidopyrene and asymmetrical

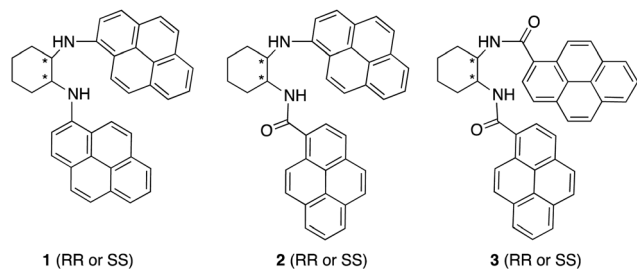
^a Univ. Bordeaux, CNRS, Bordeaux INP, ISM UMR 5255, Talence F-33400, France.

E-mail: dario.bassani@u-bordeaux.fr

^b Univ. Bordeaux, CNRS, Bordeaux INP, CBMN, UMR 5248, Pessac F-33600, France

† Electronic supplementary information (ESI) available: Synthetic details of the synthesis of compounds **1** and **2**, absorption, emission and CPL spectra. See DOI: <https://doi.org/10.1039/d3cc01802d>





Scheme 1 Structure of compounds 1–3.

amino/amidopyrene analogues (2 and 3, Scheme 1) to elucidate the origin of the CT contribution in symmetrical vs. asymmetrical excimers.

The synthesis and characterization of compounds 1–3 are detailed in the supplementary information. Briefly, 1 was obtained in 80% yield from Buchwald-Hartwig coupling of *RR*- or *SS*-*trans*-1,2-diaminocyclohexane with 1-bromopyrene whereas 2 was obtained by amidation of the mono-protected diamine with 1-pyrenecarboxylic acid followed by deprotection and arylamination. The synthesis of 3 was described previously.^{13b} The absorption spectra of 1–3 (Fig. 1) do not show appreciable signs of ground-state interactions between the chromophores. In contrast to 1 and 2, the limited solubility of 3 evidences a propensity toward aggregation that was previously noted by Liu and co-workers as being responsible for the amplification of its chiroptical properties.

The emission spectra of 1 and 3 in fluid solutions (Fig. 1) are composed of residual locally-excited (LE) emission at 390–410 nm that is characteristic of the aminopyrene or pyrene chromophore and a broad, structureless emission at longer wavelengths assigned to excimer (EX) emission.²⁰ In the case of 1 in toluene, the residual LE emission is weak and overlaps with the EX contribution. Comparing the emission of 1 and 3, it can be seen that the latter exhibits a larger proportion of EX vs. LE emission. In contrast to 1 and 3, compound 2 is non-emissive. The contribution of the long-wavelength component in the emission of 1 can be extracted by comparing the emission of 1 in nitrogen- and oxygen-saturated solutions. Because the LE

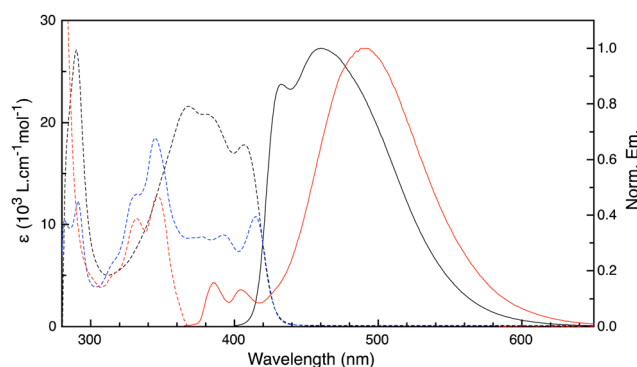


Fig. 1 Absorption (dashed lines) and emission ($\lambda_{\text{ex}} = 365$ nm, solid lines) of 1 (black), 2 (blue) 3 (red) in toluene solutions (1 μM). For 3, 5% of DMSO was added to improve solubility. No emission was detected from 2.

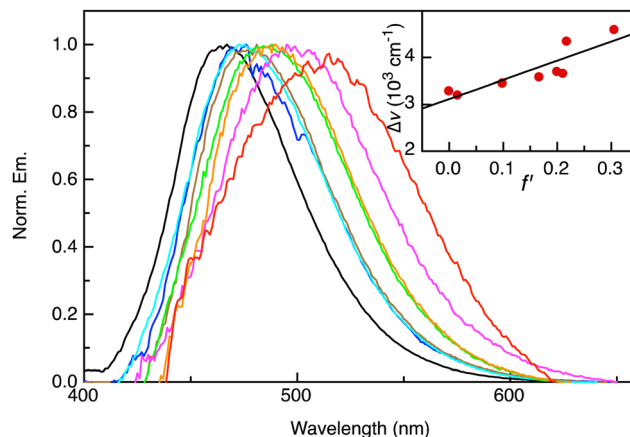


Fig. 2 Excimer contribution to the emission of 1 in various solvents obtained by subtracting the contribution from the LE state from the emission spectra. From left to right: cyclohexane, toluene, di-*n*-butylether, diethylether, ethylacetate, dichloromethane, tetrahydrofuran, acetonitrile ($\lambda_{\text{ex}} = 365$ nm). Inset shows Lippert–Mataga plot according to eqn (1) and linear best fit.

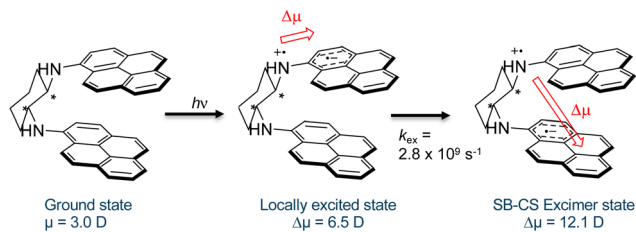
emission is short-lived, it is less sensitive to quenching by oxygen. Instead, the long-lived decay component is strongly quenched in oxygen-saturated solutions (see Fig. S3, ESI[†]). Fig. 2 shows the long-wavelength component extracted from the emission of 1 in solvents of different polarity. A shift in the emission maximum of nearly 50 nm is observed between polar and non-polar solvents. Unlike excited-state complexes (exciplexes) which possess significant CT character, the photophysical properties of excimers are largely insensitive to solvent polarity.²¹ In light of this, the strong solvatochromism observed for the long-wavelength emission of 1 is very surprising and uncommon for pyrene excimer emission. The change in dipole moment ($\Delta\mu$) between the ground and excited state can be extracted from Lippert–Mataga plots in which the emission maximum ($\bar{\nu}_{\text{max}}$) is plotted vs. the solvent polarity index ($\Delta f'$) according to eqn (2):²²

$$\bar{\nu}_{\text{max}} = \frac{2}{hca^3} \Delta f' (\Delta\mu)^2 + cst \quad (2)$$

where h is Plank's constant, a is the solvent cavity radius and $\Delta f' = \frac{\epsilon - 1}{2\epsilon + 1} - \frac{n^2 - 1}{2n^2 + 1}$ with ϵ and n being the solvent's dielectric constant and refractive index, respectively.

From the analysis of the solvent polarity dependence of the long-wavelength emission of 1, we can determine $\Delta\mu$ to be 9.1 D. Considering the dipole moment of the ground state to be 3.0 D,²³ we can estimate the dipole moment of the excited state from which the long-wavelength emission originates to be ca. 12.1 D vs. 6.5 D for the LE state. In contrast, the excimer of 3 possesses an excited-state dipole moment of only 4.2 D (see Fig. S1, ESI[†]). The broad, long-wavelength emission in 1 is absent in the parent 1-aminopyrene chromophore and can therefore be unambiguously assigned to excimer emission. That the latter possesses a greater degree of CT character with respect to the LE state indicates that the CT character of the LE





Scheme 2 Proposed sequential CT steps leading to SB-CS upon excitation of **1**.

state is further increased upon excimer formation. This can best be rationalized by the occurrence of (partial) CT stabilization in the excimer, as illustrated in Scheme 2.

Symmetry-breaking charge separation (SB-CS) in excimers has been most commonly observed in perylene derivatives, where it results from fluctuations of the solvation sphere that lead to desymmetrization of the electronic environment of the excited state.²⁴ This is not likely the case in **1**, where the LE state already possesses CT character and excimer formation is slow with respect to solvent fluctuations. A rate of $k_{\text{ex}} = 2.8 \times 10^9 \text{ s}^{-1}$ (cyclohexane solution) can be determined from the decrease in the LE state lifetime with respect to the parent chromophore. The second diabatic CT step in **1** is thermodynamically favored based on the excimer stabilization energy estimated from the difference in emission maxima between the LE and excimer emission ($\Delta E = -0.37 \text{ eV}$). The involvement of a CT mechanism seems probable considering the redox potentials of the parent chromophore: In DMF, 1-aminopyrene undergoes irreversible oxidation at 0.67 V and quasi-reversible reduction at -0.77 V . According to the Weller equation,²⁵ we may estimate photo-induced electron transfer yielding a radical ion pair to be favored even in a non-polar solvent such as cyclohexane, where $\Delta G_{\text{rip}} = -0.32 \text{ eV}$.[‡]

The behavior of **1** can be compared to that of **3**, for which excimer emission is also observed. The latter, however, shows only minor solvent polarity dependence as indicated by a shift in the emission maximum of only 10 nm between polar and non-polar solvents. An excited state dipole moment of $\mu = 5.3 \text{ D}$ is found from the Lippert–Mataga plot (see supplementary information). This indicates that the excimer in **3** possesses little or no CT character in contrast to that of **1**.

The situation for **2** differs from that of **1** or **3** in that this compound is not fluorescent. Photoinduced intramolecular electron transfer from the aminopyrene in **2** to the amidopyrene moiety is expected to be exothermic but, unlike in **1**, the resulting CT state is non-emissive. Similar behavior was observed for the formation of a non-emissive exciplex between 1-aminopyrene and pyridine which was also found to possess strong CT character.²⁶ In **2**, this could be due to either poor orbital overlap resulting from the different linker geometries of the two aromatic moieties or, more likely considering the lack of LE emission, to fast back electron transfer repopulating the ground state.

The unusually strong emission of **1** is surprising for SB-CS species which are typically non-emissive.²⁷ Kim, Würthner, and

Table 1 Photophysical data for **1** in various solvents^a

Solvent	Φ_{F}^b	$\Phi_{\text{F}}(\text{LE})^c$	$\Phi_{\text{F}}(\text{EX})^d$	$\lambda(\text{LE})^{-1cd}$	$\lambda(\text{EX})^{-1de}$	g_{lum}^f
Cyclohexane	0.33	0.13	0.20	0.33	14.8	0.016
Toluene	0.31	0.17	0.14	0.16	18.7	0.016
Et ₂ O	0.28	0.16	0.12	0.25	15.8	
AcOEt	0.21	0.14	0.07	0.37	16.6	
THF	0.45	0.34	0.11	0.54	19.9	
CH ₂ Cl ₂	0.21	0.14	0.07	0.14	22.0	0.017
CH ₃ CN	0.09	0.06	0.03	0.08	17.6	

^a Degassed solutions (conc. = 10^{-6} M). ^b Total fluorescent quantum yield ($\lambda_{\text{ex}} = 365 \text{ nm}$). ^c Assigned to LE contribution. ^d In ns. ^e Assigned to EX contribution. ^f 50 μM solution.

co-workers observed weak excimer fluorescence ($\Phi_{\text{F}} \leq 0.06$) in a cofacial perylene bisimide cyclophane that underwent SB-CS.²⁸ They showed that the excimer state is an intermediate preceding the formation of the CS state and that its emission does not exhibit appreciable solvent polarity dependence. Similarly, Hariharan and co-workers found that excimer formation in orthogonal core-annulated perylenediimide dimers occurs in competition with SB-CS.²⁹

The situation is markedly different for **1** in that the emission of the excimer contribution is significant in both polar and non-polar solvents (Table 1). Furthermore, the linearity of the Lippert–Mataga plot suggests that the CT nature and geometry of the excimer are preserved in both polar and non-polar solvents. The decay of the fluorescence emission in **1** can be described by a tri-exponential function whose short and long-lived decays are assigned respectively to emission from the LE and EX states, respectively. A minor third decay component, similar to that of 1-aminopyrene, is also found and, in agreement with previous studies by De Schryver and co-workers on the kinetics of intramolecular excimer formation in 1,3-di(1-pyrenyl)propane,^{20,21} it is assigned to emission from **1** in a geometry that is not amenable to excimer formation within the excited-state lifetime.

The emission of **1** exhibits strong circular polarization in both polar and non-polar solvents (Fig. 3). Interestingly, two regions are observed, corresponding to the emission from the LE and EX states. The CPL signal from the LE state, at shorter wavelengths, is weak with a $g_{\text{lum}} = 10^{-3}$ that is typical of small molecule emitters. Instead, the broad, structureless signal observed at longer wavelengths exhibits a strong CPL signal with $g_{\text{lum}} = 1.6 \times 10^{-2}$. The value of the emission of maximum CPL signal corresponds to the λ_{max} of the emission assigned to the SB-CS excimer state in solvents of different polarity, indicating that the latter is responsible for the CPL signal. Furthermore, we can see that the magnitude of the dissymmetry factor is insensitive to solvent polarity, corroborating the assertion that no significant change in the emissive EX geometry occurs between polar and non-polar solvents. The CPL brilliance (B_{CPL}) has been proposed by Zinna and co-workers as a metric to compare CPL emitters.³ For **1** in THF, we find $B_{\text{CPL}} = 190 \text{ M}^{-1} \text{ cm}^{-1}$ (365 nm), which is comparable to binaphthalene multi-chromophore assemblies and significantly higher than the median ($43.2 \text{ M}^{-1} \text{ cm}^{-1}$) for this class of compounds.³



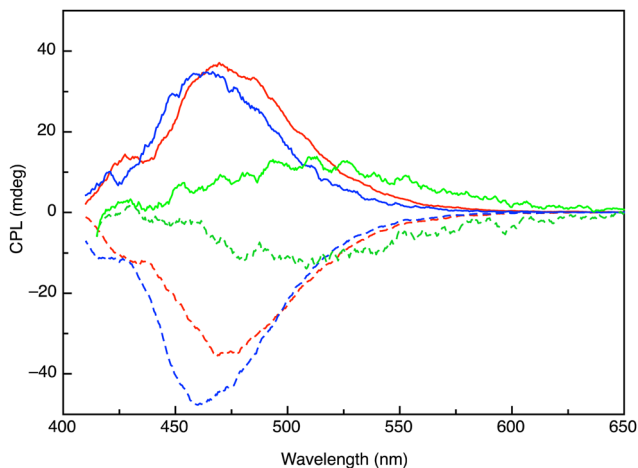


Fig. 3 Circularly polarized luminescence from the SS (solid lines) and RR (dashed lines) enantiomers of **1** in Ar-purged cyclohexane (blue), toluene (red) and dichloromethane (green) solutions (conc. = 50 μ M, λ_{ex} = 365 nm).

To the best of our knowledge, the behavior of **1** is unique in providing the first example of an emissive SB-CS excimer state exhibiting strong CPL emission. Although CPL from pyrene excimers is well-documented, these possess little or no CT character as a result of their non-polar ground and excited states. The advent of charge separation therefore provides an alternative strategy to improve CPL compared to reinforcing the chiral environment of the chromophore through aggregation (as in **3**) or by multi-chromophore constructs. Clearly, there is a subtle energetic balance that must be considered in rendering the CS state thermodynamically favorable without inducing too much stabilization that facilitates internal conversion to the ground state. Increasing the driving force for CS (as in **2**) results in a chromophore that is no longer emissive due to fast forward and return electron transfer. Understanding this balance can provide a means to further improve the CPL properties of small organic molecules by harnessing charge separation.

This work was supported by the CNRS and the University of Bordeaux. We acknowledge the financial support from the ANR through project ANR-21-CE09-0012-01 and expertise of the CESAMO platform UMR 5255, supported by the Nouvelle-Aquitaine region.

Conflicts of interest

There are no conflicts to declare.

Notes and references

‡ The same calculation applied to pyrene gives the formation of a radical ion pair in cyclohexane to be endothermic by 1.14 eV.

- (a) S. Felder, M.-L. Delcourt, D. Contant, R. Rodriguez, L. Favereau, J. Crassous, L. Micouin and E. Benedetti, *J. Mater. Chem. C*, 2023, **11**, 2053–2062; (b) S.-P. Wan, H.-Y. Lu, M. Li and C.-F. Chen, *J. Photochem. Photobiol., C*, 2022, **50**, 100500.
- R. P. Cameron, J. B. Götte, S. M. Barnett and A. M. Yao, *Philos. Trans. Royal Soc. A*, 2017, **375**, 20150433.
- L. Arrico, L. Di Bari and F. Zinna, *Chem. – Eur. J.*, 2021, **27**, 2920–2934.
- H. Tanaka, Y. Inoue and T. Mori, *ChemPhotoChem*, 2018, **2**, 386–402.
- Y. Nagata and T. Mori, *Front. Chem.*, 2020, **8**, 448.
- (a) T. Mori, *Chem. Rev.*, 2021, **121**, 2373–2412; (b) H. Kubo, T. Hirose, T. Nakashima, T. Kawai, J.-Y. Hasegawa and K. Matsuda, *J. Phys. Chem. Lett.*, 2021, **12**, 686–695.
- K.-I. Sugiura, *Front. Chem.*, 2020, **8**, 700.
- (a) K. Takaishi, R. Takehana and T. Ema, *Chem. Commun.*, 2018, **54**, 1449–1452; (b) K. Takaishi, K. Iwachido, R. Takehana, M. Uchiyama and T. Ema, *J. Am. Chem. Soc.*, 2019, **141**, 6185–6190.
- Y. Ohishi and M. Inouye, *Tetrahedron Lett.*, 2019, **60**, 151232.
- (a) K. Takaishi, S. Murakami, F. Yoshinami and T. Ema, *Angew. Chem., Int. Ed.*, 2022, **61**, e202204609; (b) H. Shigemitsu, K. Kawakami, Y. Nagata, R. Kajiwara, S. Yamada, T. Mori and T. Kida, *Angew. Chem., Int. Ed.*, 2022, **61**, e202114700.
- A. Homberg, E. Brun, F. Zinna, S. Pascal, M. Gorecki, L. Monnier, C. Besnard, G. Pescitelli, L. Di Bari and J. Lacour, *Chem. Sci.*, 2018, **9**, 7043–7052.
- C. Xue, L. Xu, H.-X. Wang, T. Li and M. Liu, *ChemPhotoChem*, 2022, **6**, e202100255.
- (a) S. Ito, K. Ikeda, S. Nakanishi, Y. Imai and M. Asami, *Chem. Commun.*, 2017, **53**, 6323–6326; (b) S. Hu, L. Hu, X. Zhu, Y. Wang and M. Liu, *Angew. Chem., Int. Ed.*, 2021, **60**, 19451–19457; (c) Y. Zhang, H. Li, Z. Geng, W. Zheng, Y. Quan and Y. Cheng, *Nat. Commun.*, 2022, **13**, 4905.
- C. Li, X. Jin, J. Han, T. Zhao and P. Duan, *J. Phys. Chem. Lett.*, 2021, **12**, 8566–8574.
- J. B. Birks, *Photophysics of aromatic molecules*, Wiley-Interscience, London, 1970.
- K. Takaishi, S. Murakami, K. Iwachido and T. Ema, *Chem. Sci.*, 2021, **12**, 14570–14576.
- N. Dhbaibi, L. Abella, S. Meunier-Della-Gatta, T. Roisnel, N. Vanthuyne, B. Jamoussi, G. Pieters, B. Racine, E. Quesnel, J. Autschbach, J. Crassous and L. Favereau, *Chem. Sci.*, 2021, **12**, 5522–5533.
- H. Miyasaka, A. Tabata, K. Kamada and N. Mataga, *J. Am. Chem. Soc.*, 1993, **115**, 7335–7342.
- M. Coehlo, G. Clavier and G. Pieters, *Adv. Opt. Mater.*, 2022, **10**, 2101774.
- F. C. De Schryver, P. Collart, J. Vandendriessche, R. Goedeweeck, A. M. Swinnen and M. Van der Auweraer, *Acc. Chem. Res.*, 1987, **20**, 159.
- J. B. Birks, *Nature*, 1967, **214**, 1187–1190.
- N. Mataga, Y. Kaifu and M. Koizumi, *Bull. Chem. Soc. Jpn.*, 1955, **28**, 690–691.
- H. Orucu and N. Acar, *J. Mol. Struct.*, 2018, **1174**, 43–51.
- B. Dereka, D. Svehkarev, A. Rosspeintner, A. Aster, M. Lunzer, R. Liska, A. M. Mohs and E. Vauthey, *Nat. Commun.*, 2020, **11**, 1925.
- A. Weller, *Z. Phys. Chem.*, 1982, **133**, 93–98.
- N. Ikeda, H. Miyasaka, T. Okada and N. Mataga, *J. Am. Chem. Soc.*, 1983, **105**, 5206.
- E. Sebastian and M. Hariharan, *ACS Energy Lett.*, 2022, **7**, 696–711.
- J. Sung, A. Nowak-Król, F. Schlosser, B. Fimmel, W. Kim, D. Kim and F. Würthner, *J. Am. Chem. Soc.*, 2016, **138**, 9029–9032.
- E. Sebastian, J. Sunny and M. Hariharan, *Chem. Sci.*, 2022, **13**, 10824–10835.

